A Radially and Rotationally Adjustable Magnetic Mangle for Electron Beams

Ishaan Vohra, Isabella Vesely, Peter Morand, Aubrey Zhang, William Lu, William Soh, Achyuta Rajaram, Daniel Jeon

Myriad Magnets

Phillips Exeter Academy, Exeter, NH, USA

A Radially and Rotationally Adjustable Magnetic Mangle for Electron Beams

Contents

1 Introduction

Excessive energy usage is a major contributor to climate change, a pressing world issue [1]. Electromagnets used at accelerator facilities can consume large quantities of energy – it is therefore worthwhile to investigate alternative technologies that provide the same capabilities.

We propose a multifunctional variant of the Halbach cylinder known as a magnetic mangle [2, 3], designed for 0.5 – 6 GeV electron beams[1]. Our mangle can be radially adjusted to achieve a continuous range of interior magnetic flux densities, and rotationally adjusted to switch between generating dipole and quadrupole fields. Similar to conventional Halbach cylinders, our magnetic mangle produces a strong magnetic field inside the array while generating very weak magnetic fields externally, making it safer to use near other electronics (such as cellphones, detectors, or pacemakers) than typical magnet setups.

In our experiment, we aim to demonstrate the viability of our mangle design. We hope that our design and experiment will act as a proof of concept for future electromagnet alternatives in accelerators.

2 Why we want to go

As passionate physics students, going to CERN/DESY will bring us amazing insights into particle physics first-hand, allowing us to work with cutting edge equipment alongside experts. We are very eager to turn our proposal into a reality as we strongly believe that our design will help make future particle physics experiments safer and more sustainable.

3 Aim of the experiment

We aim to validate our magnetic mangle's ability to bend and focus electron beams in the 0.5 – 6 GeV range. We will compare the observed electron deflection distributions with our simulated deflection distributions in GEANT4 to analyze how well our predictions align with the real performance of the magnet [4]. We also aim to further investigate any discrepancies that arise between the experiment and simulation.

4 Magnet design

4.1 Adjustable magnetic mangle

A magnetic mangle consists of N permanently diametrically-magnetized cylinders arranged in a circle such that the desired flux density and polarity is achieved in

[1] We have chosen to design our mangle for electrons over other charged particles because both CERN and DESY can provide high purity electron beams (see Section 5).

the central cavity, while only a very weak flux density is produced externally [5]. One rotational arrangement of the cylinders creates a dipole field in the cavity, while another creates a quadrupole field (see Figure 1). Moreover, by moving each cylinder radially outward or inward from the center of the array, the flux density within the cavity can be decreased or increased, respectively.

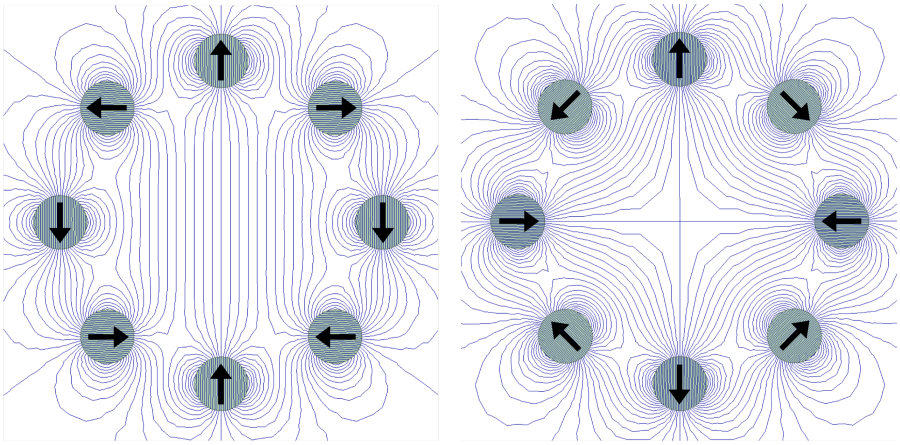

(a) Dipole arrangement (b) Quadrupole arrangement

Figure 1: Simulated flux diagrams of the dipole and quadrupole rotational arrangements for $N = 8$ cylinders. Black arrows denote the direction of magnetization of each cylinder.

Since magnetic mangles consist of a finite number of cylinders with fixed directions of magnetization, the fields they generate deviate from ideal dipole and quadrupole fields, as can be seen near the edges of the interior field in Figure 1. In general, as N increases, the deviation from the ideal field decreases, improving the accuracy with which electrons are deflected. However, if too many cylinders are used, it becomes impractical to rotate each one between configurations.[2]

To optimally balance these two factors, we used the ANSYS Maxwell simulation software [6] to model 2D cross-sections of mangles with various N. The deviation of each mangle field from the corresponding ideal field (see Appendix Section 10.1) was quantified using the relative absolute error (RAE) given by

$$\text{RAE} = \frac{\sqrt{\sum_{i=1}^{n} |\vec{B}_{mangle_i} - \vec{B}_{ideal_i}|^2}}{\sqrt{\sum_{i=1}^{n} |\vec{B}_{ideal_i}|^2}}, \tag{1}$$

[2]Our mangle design provides the flexibility to individually rotate each cylinder to allow for magnetic field arrangements other than dipole and quadrupole.

where $\vec{B}_{mangle_i}$ and $\vec{B}_{ideal_i}$ are the mangle field and corresponding ideal field vectors at a given sample point i out of n total sample points. The results of the analysis are shown below in Figure 2.

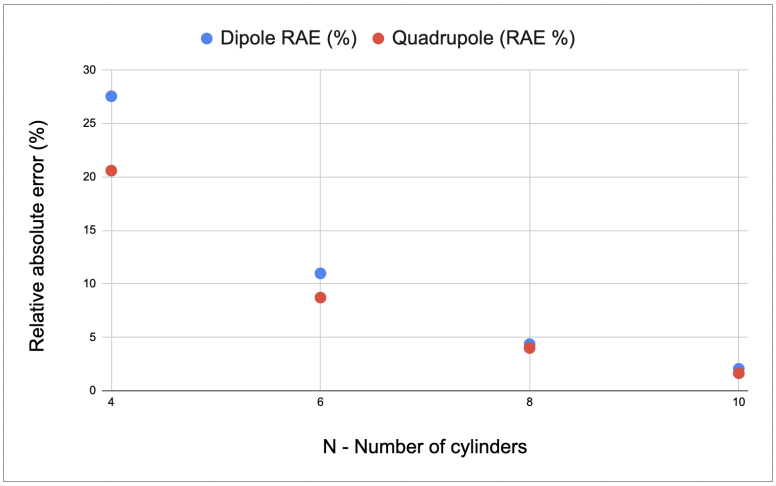

Figure 2: Plot of the RAE for 2D cross-sections of magnetic mangles with different numbers of cylinders.

As shown, $N = 8$ is the fewest number of cylinders needed to have both dipole and quadrupole RAE under 5%. Thus, we opted for 8 cylinders, allowing the mangle to generate fields that do not deviate much from the ideal while maintaining rotation efficiency.

We then conducted a cost analysis based on the experiment budget and settled on the design shown in Figure 3.

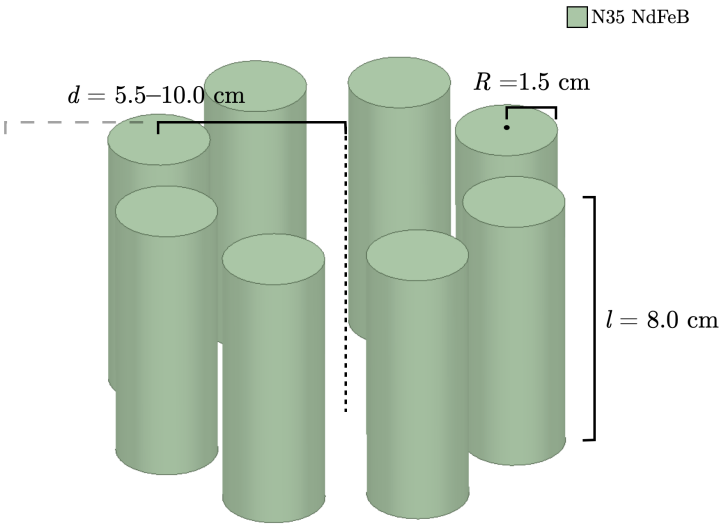

Figure 3: Simulated design of our magnetic mangle to be constructed using N35-grade NdFeB. We aim to use sustainably-sourced rare-earth metals in order to minimize the environmental footprint of the experiment.

The radial adjustment range of $d = 5.5$–10.0 cm considers not only the 5x5 cm minimum cavity size, but also the coercivity limit of typical N35 NdFeB magnets – according to our simulations, this range provides a 20% margin between the maximum flux density experienced by any part of the mangle and the magnets' $\mu_0 H_c \approx 1.2$T. Above this limit, the cylinders' directions of magnetization may change undesirably.

For more detail on the expected cost and sourcing of the mangle's components, refer to our cost analysis.[3]

Further simulations of the final mangle design were also performed (see Figures 4 and 5) to model B, the dipole flux density, and g, the quadrupole flux density gradient, for different values of d, as well as to demonstrate that the external field grows weaker with increasing distance. Prior to installing the mangle in the beamline, we intend to measure its field pattern in different configurations using a magnetometer to compare against the simulated results.

[3] See our cost analysis spreadsheet at: https://docs.google.com/spreadsheets/d/1oWpocO46t6OGfqjlob-5VgnrV-Hy8mJZ3GOcQm68XXM/edit?usp=sharing

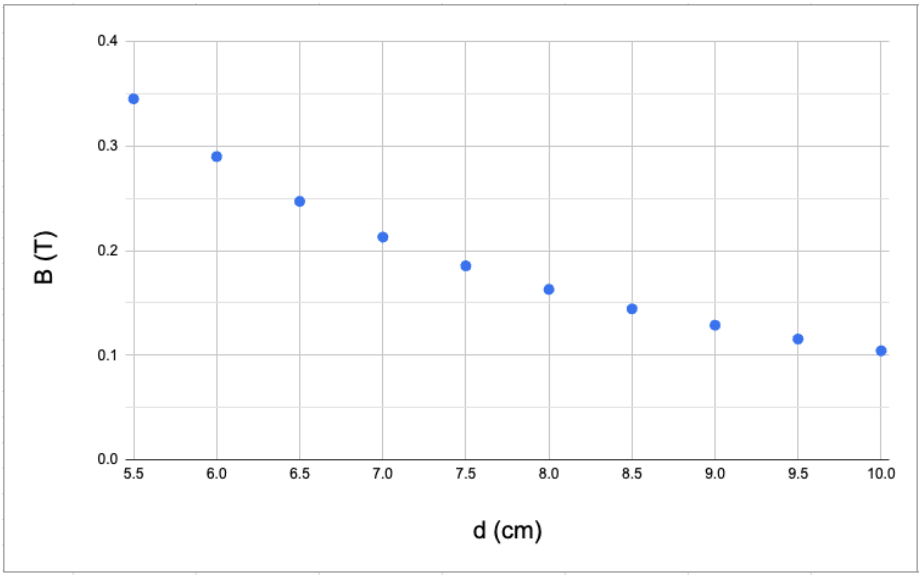

(a) Dipole: magnetic flux density magnitude (sampled from center of cavity) for different radial distances of the cylinders.

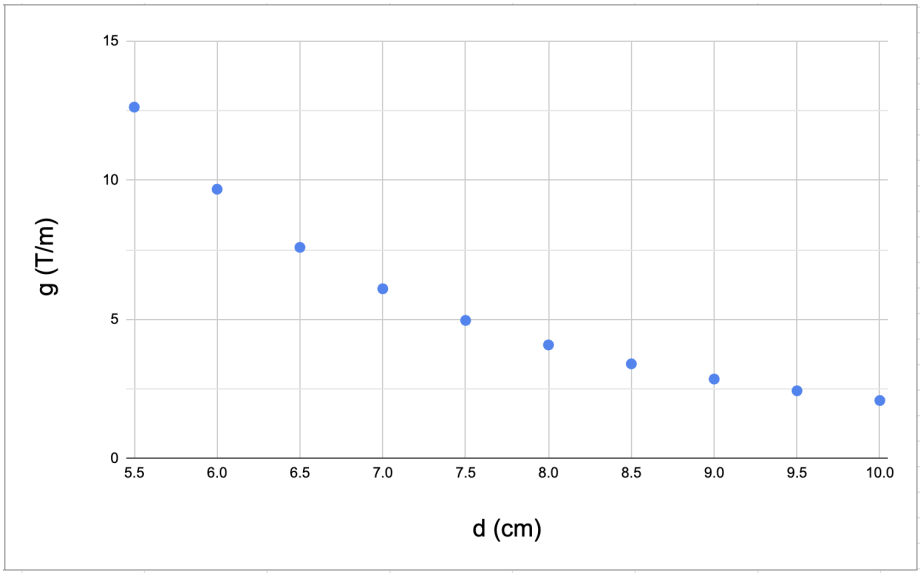

(b) Quadrupole: magnetic flux density gradient for different radial distances of the cylinders.

Figure 4: Flux density and flux density gradient plots for different dipole and quadrupole radial configurations in the final mangle design.

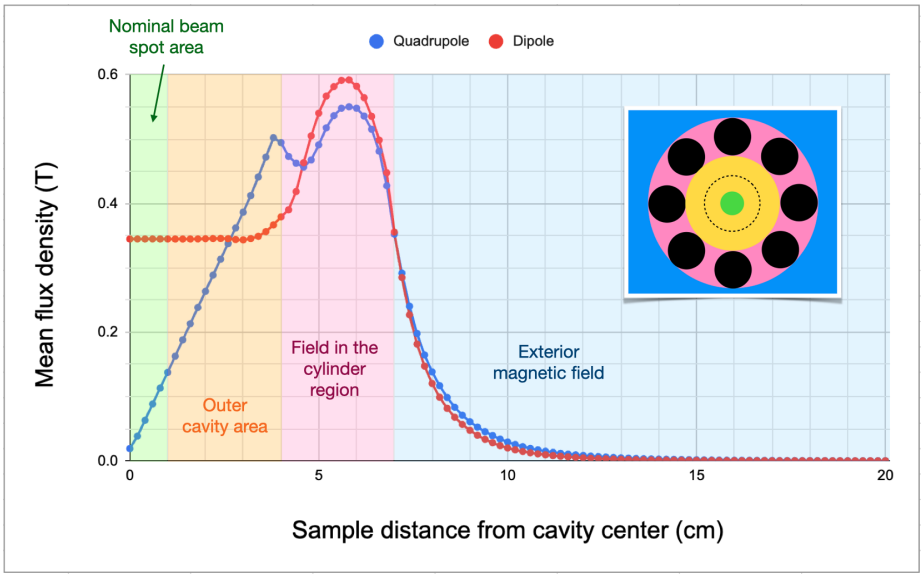

Figure 5: Mean flux density at a given radial sample distance from the cavity center for dipole and quadrupole configurations with $d = 5.5$ cm. As shown by the dotted black line in the top right diagram, the mean flux density at a given radial distance is found by uniformly sampling points around a circular ring and averaging the flux density. As seen in the blue region, the exterior flux density decreases to about 0.2 mT within 20 cm from the cavity center – this is a level considered safe for most electronic devices.

4.2 Brace structure

Our brace structure (Figures 6 and 7) enables continuous radial adjustments and rotational freedom around the magnets' central axes. A radial linkage translates the magnets and may be manually adjusted by shortening and extending four aluminum turnbuckle-style rods connecting the moving pin joints. We determined through our simulations that the magnets exert up to 350 N of radially-directed force and 4 Nm of torque on each other; the titanium brace structure has thus been designed to withstand this. The linkage structure itself is attached to a 76.2 mm-thick standing block of ultra high molecular weight polyethylene, providing cost-efficient stability. Since polyethylene is non-magnetic and aluminum and titanium are only weakly paramagnetic, we expect the brace structure to have a negligible effect on the mangle's magnetic field. For a description of how the magnets can be rotated, see Appendix Section 10.2.

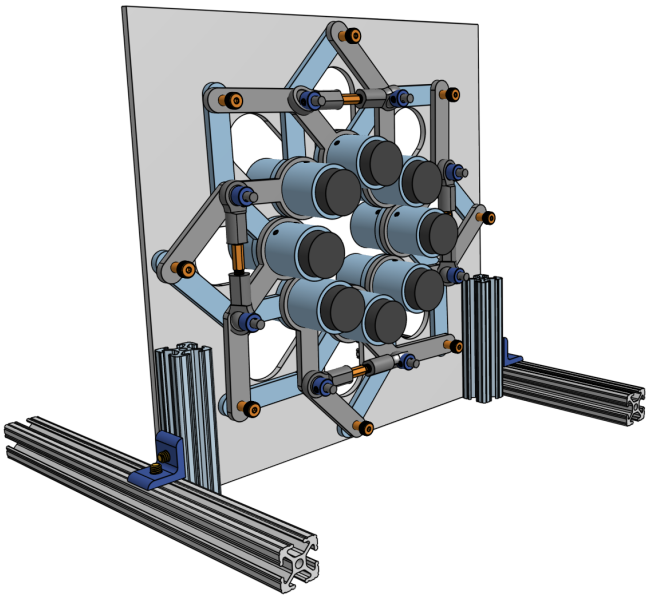

Figure 6: CAD design of the brace structure with magnets in place: magnets (black) are attached to the inner linkage joints through aluminum casings (blue). Set screws are installed optimally along the axial line and at a 60° displacement angle, applying friction and thus restricting rotational freedom to any chosen angle and allowing for both dipole and quadrupole arrangements in any direction.

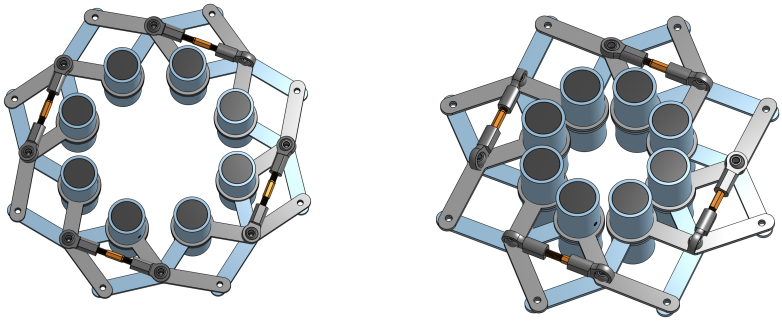

(a) 9.2 cm radius arrangement

(b) 5.6 cm radius arrangement

Figure 7: Two configurations for varied radii. The orange, turn-buckle style rods can be screwed and unscrewed to adjust their length, thus adjusting the magnets' distance from center.

5 Experiment design

To minimize the number of stray particles in our beam, we plan to use either the 0.5–4 GeV high-purity electron beam at CERN or the 1–6 GeV electron beam at DESY [7].

5.1 Detector setup

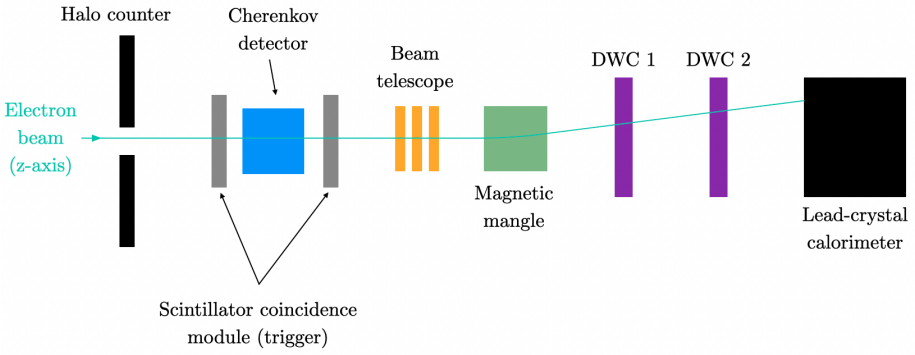

Figure 8: Detector setup to measure the electron deflection through the magnetic mangle.

- Before entering the mangle, the beam telescope measures the incoming angle of electrons with high spatial resolution. At this stage, the beam spot is only about 2 cm in diameter, so the beam will pass within the 2x2 cm sensor area.
- Two DWC's track the positions of electrons deflected by the magnetic mangle. The first DWC is placed near the mangle and the second is placed further away to study the beam divergence and the deflection due to the magnet.
- Data from the Cherenkov detector, halo counter, and calorimeter can be used to filter events during data analysis (see Section 5.3).

5.2 Schedule

We plan to run our experiment in about 9 days with the following schedule:

- Days 1-4: Set up experiment, align detectors, integrate the DAQ.
- Day 5: Control run with detectors but without magnetic mangle (to study intrinsic beam divergence).
- Day 6: Dipole configuration at 4 energies.

- Day 7: Dipole configuration (with a radial adjustment) at the same 4 energies.
- Day 8: Quadrupole configuration at 4 energies.
- Day 9: Quadrupole configuration (with a radial adjustment) at the same 4 energies.

During the following days, we could analyze data and conduct additional runs if necessary. Extra runs could involve the same above setups, or if time permits, we could investigate the electron deflections using other angular configurations besides dipole and quadrupole, such as a field that both bends and focuses electrons (a gradient magnet).

5.3 Data analysis

Each event is analyzed particle-by-particle. Halo counter data is first used to filter out any uncollimated stray particles. Although the electron beam is known to be of high purity, the Cherenkov detector is used to tag and filter out remaining pions or muons.

Calorimeter data is used to reject electrons which have lost $\gtrsim$ 100MeV.[4] These electrons may have collided with the air and changed direction or lost too much energy emitting synchrotron radiation in the mangle's magnetic field (among other effects). Such backgrounds and mechanisms of energy loss would cause erroneous signals in the DWCs, and would therefore need to be filtered out.

From the remaining electron deflection events, plots are created to characterize the observed deflections over different energies and mangle configurations. The plots can then be compared to the simulated plots in GEANT4 (Figures 9 and 10) to assess the true performance of our mangle.

[4] 100 MeV is a temporary estimate for the energy threshold of the DWCs – this value may be adjusted when better understood.

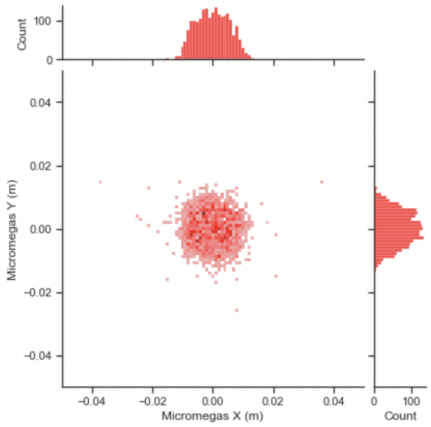

(a) No magnetic mangle present in beamline

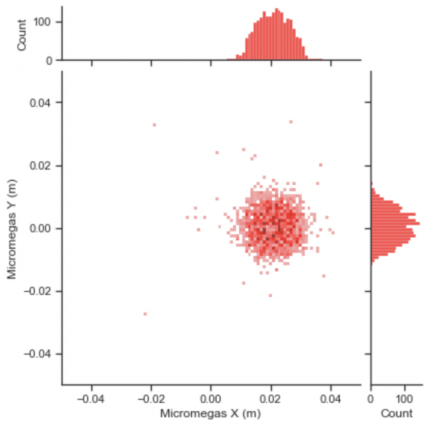

(b) Dipole configuration with radial arrangement of $d = 6.0$ cm ($B = 0.29$ T)

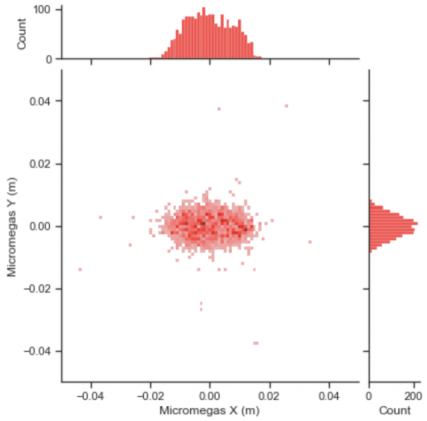

(c) Quadrupole configuration with radial arrangement of $d = 7.0$ cm ($g = 6.1$ T/m)

Figure 9: GEANT4 simulation: position distributions of 1500 electrons on a tracking detector 4.9 m from the mangle. The plots were simulated using a circular particle source 2 cm in diameter and a simplified detector volume for the tracking detector.

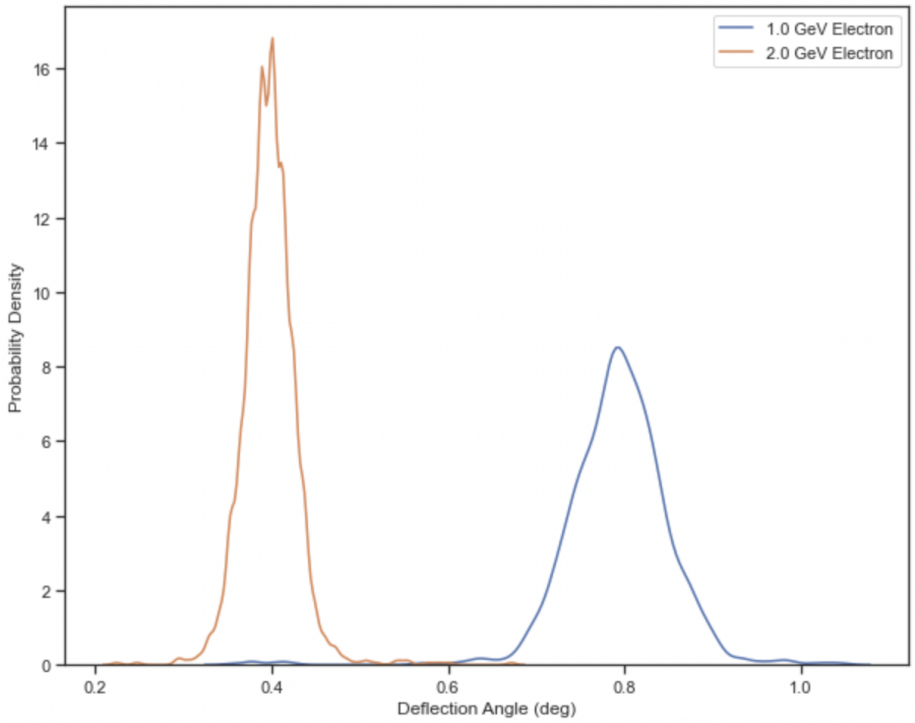

Figure 10: GEANT4 simulation: Normalized deflection angle distributions at 1.0 GeV and 2.0 GeV passing through the mangle dipole configuration.

6 What we hope to take away from the experience

Working on this project has proven invaluable to our development as budding physicists. As we complete our research, we are gaining first-hand exposure to the practical considerations, physics knowledge, and dedication involved in improving energy efficiency at the bleeding edge of high-energy science. Additionally, by collaborating with the researchers at CERN and DESY, we hope to learn invaluable skills that we can use throughout our scientific careers.

7 Outreach activity

We hope to extend our efforts to visit local elementary and middle schools to expose younger students to STEM. We plan to collaborate with our school's service organization to organize these events, making use of their close connections with the local libraries and primary schools. We plan to foster curiosity and excitement in physics by holding approachable physics conversations, focusing

on concepts rather than math. By leading engaging and easily understandable talks, we hope to inspire the next generation of scientists.

We also plan on holding several talks through our physics club about our proposal. We will prioritize reaching out to members of our school community who are not yet involved in science clubs through social media, posters, and word of mouth.

8 Acknowledgements

We would like to sincerely thank our physics teachers, Mr. James DiCarlo and Mr. Scott Saltman for granting us permission to compete in the Beamline for Schools Competition and for supporting our project. We are also extremely grateful to Dr. Mark Adams, Dr. Don Lincoln, Dr. Elvin Harms Jr, Dr. Josh Barrow, and Mr. Daniel MacLean (all of Fermilab) for guiding us along the way with their valuable advice. We would also like to thank Dr. Efstathios Stefanidis (former ATLAS physicist), Dr. Rasmus Bjork (of the Denmark Technical University), and Dr. Marco Roda (of the University of Liverpool) for their guidance and support. This proposal also would not have been possible without the assistance of Dr. Markus Joos and Dr. Margherita Boselli (of BL4S) who swiftly answered all of our questions, as well as Mr. Kenneth Cecire, the United States national contact for the Beamline for Schools Competition. Lastly, we would like to thank our school, Phillips Exeter Academy, for providing us with an exceptional learning environment to pursue our passion for physics.

9 References

[1] K. Gillingham, R. G. Newell, and K. Palmer, "Energy efficiency economics and policy," *Annu. Rev. Resour. Econ.*, vol. 1, no. 1, pp. 597–620, 2009.

[2] R. Bjørk, C. R. H. Bahl, A. Smith, and N. Pryds, "Optimization and improvement of halbach cylinder design," *Journal of Applied Physics*, vol. 104, no. 1, p. 013910, 2008.

[3] C. Fernandes, J. Ventura, and D. Silva, "Rod mangle rotation patterns for adjustable magnetic field generation," *Journal of Magnetism and Magnetic Materials*, vol. 565, p. 170227, 2023.

[4] S. Agostinelli, J. Allison, K. a. Amako, J. Apostolakis, H. Araujo, P. Arce, M. Asai, D. Axen, S. Banerjee, G. Barrand, *et al.*, "Geant4—a simulation toolkit," *Nuclear instruments and methods in physics research section A: Accelerators, Spectrometers, Detectors and Associated Equipment*, vol. 506, no. 3, pp. 250–303, 2003.

[5] H. A. Leupold, "Mangle magnetic structure," Apr. 23 2002. US Patent 6,376,959.

[6] A. S. Martyanov and N. I. Neustroyev, "Ansys maxwell software for electromagnetic field calculations," *Eastern European Scientific Journal*, no. 5, 2014.

[7] "Beams and detectors."

10 Appendix

10.1 Defining the corresponding ideal field

For each set of cross-sectional mangle fields with a given N, we define the corresponding ideal fields (centered at the origin) to be

$$\vec{B}_{dip}(x, y) = [0, B] \tag{2}$$

in the dipole case and

$$\vec{B}_{quad}(x, y) = g[-x, y] \tag{3}$$

in the quadrupole case. The magnitude of the ideal dipole's flux density, B, is obtained from the flux density at the center of the array. The ideal quadrupole's magnetic flux gradient, g, is obtained through a linear regression of the flux density magnitude plotted against sample distance from the center of the cavity.

For each mangle field, thousands of coordinates were sampled uniformly from a circular area of the cavity with radius 3.54 cm (corresponding to the circumcircle of the 5x5 cm minimum cavity size through which the electron beam

passes). From these coordinates, the RAE was then calculated to quantify the deviation of the mangle field from the corresponding ideal field (see Section 4.1).

10.2 Rotating the magnets

To rotate the magnets, the mangle is first set to its largest radial configuration ($d = 10.0$ cm) to reduce the forces and torques between the magnets. Custom cranks are attached to each magnet and tightened with a set screw; the magnet casing is then loosened, and the crank rotates them to the desired rotational configuration. Markings on the casing align with the magnets' markings at common angle intervals (every 5°).

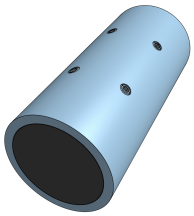

(a) Casing with all four set screws visible

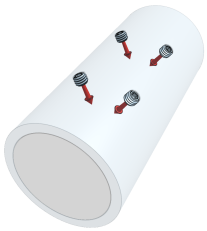

(b) Set screws inside the casing